

GSURS: Generalized Sparse Uniform ReSampling with Application to MRI

Amir Kiperwas

Department of Electrical Engineering
Technion, Israel Institute of Technology
Email: amirki@tx.technion.ac.il

Daniel Rosenfeld

RAFAEL
Advanced Defense Systems Ltd., Israel
Email: danielr@rafael.co.il

Yonina C. Eldar

Department of Electrical Engineering
Technion, Israel Institute of Technology
Email: yonina@ee.technion.ac.il

Abstract—We present an algorithm for resampling data from a non-uniform grid onto a uniform grid. Our algorithm termed generalized sparse uniform resampling (GSURS) uses methods from modern sampling theory. Selection of an intermediate subspace generated by integer translations of a compactly supported generating kernel produces a sparse system of equations representing the relation between the nonuniformly spaced samples and a series of generalized samples. This sparse system of equations can be solved efficiently using a sparse equation solver. A correction filter is subsequently applied to the result in order to attain the uniformly spaced samples of the signal. We demonstrate the application of the new method for reconstructing MRI data from nonuniformly spaced k-space samples. In this scenario, the algorithm is first used to calculate uniformly spaced k-space samples, and subsequently an inverse FFT is applied to these samples in order to obtain the reconstructed image. Simulations using a numerical phantom are used to compare the performance of GSURS with other reconstruction methods, in particular convolutional gridding and the nonuniform FFT.

I. INTRODUCTION

Medical imaging systems such as magnetic resonance imaging (MRI) and computerized tomography (CT) sample signals in k-space, namely the spatial frequency domain. A non-Cartesian sampling grid in k-space is often used to improve acquisition time and efficiency. A popular approach to recover the original image is to resample the signal on a Cartesian grid and then use the inverse fast Fourier transform (IFFT) in order to transform back into the image domain. It has been shown [1] that this is advantageous in terms of the computational complexity involved.

In MRI, the most widely used resampling algorithm is convolutional gridding (CG) [2], which consists of four steps: 1) precompensation for varying sampling density; 2) convolution with a Kaiser-Bessel window onto a Cartesian grid; 3) IFFT; and 4) postcompensation by dividing the image by the transform of the window.

Two other notable classes of resampling methods employed in medical imaging are the least-squares (LS) and the nonuniform-FFT (NUFFT) algorithms. LS methods, in particular URS/BURS [3], [4], exploit the relationship between the acquired nonuniformly spaced k-space samples and their uniformly spaced counterparts, as given by the standard sinc-function interpolation of the sampling theorem. These methods invert this relationship using the regularized pseudo-inverse.

The NUFFT [5], [6] is a computationally efficient family of algorithms for approximating the inverse Fourier transform directly from the nonuniformly spaced samples. These methods first define a “forward problem” which performs the Fourier transform from the image domain to the nonuniformly spaced samples in k-space by approximating efficiently a nonuniform Fourier matrix [7]. Next, the adjoint of the forward problem is calculated. Finally, using a variant of the conjugate gradient method, these two operations are executed iteratively until convergence of the result is achieved.

In recent years the concepts of sampling and reconstruction were generalized within the mathematical framework of function spaces [8]. Methods were developed for reconstructing a desired signal, or an approximation of this signal, beyond the restrictions of the Shannon-Nyquist sampling theorem.

In this paper we apply these concepts to the problem of reconstruction of MRI or CT images from nonuniformly spaced measurements in k-space. The proposed method is compared with other prevalent reconstruction methods in terms of its accuracy, its computational burden and its behaviour in the presence of noise, and is shown to produce excellent results.

II. PROBLEM FORMULATION

An MRI image is represented by a gray level function $F(x)$, where x denotes the spatial coordinate (in 2 or 3 spatial dimensions). The Fourier transform of the image function is denoted $f(k)$, where k is the spatial frequency domain coordinate, termed k-space:

$$f(k) = \int_{-\infty}^{\infty} F(x) e^{-ik2\pi x} dx.$$

The MRI tomograph collects a finite number of k-space raw data samples $f(\kappa_m)$, $m = 1, \dots, M$ where the sampling points $\{\kappa_m\}$ may be nonuniformly distributed in k-space. These samples are arranged in a vector \mathbf{b} , where $b[m] = f(\kappa_m)$. In MRI, the field of view (FOV) in the image domain is limited, which implies that $f(k)$ is represented by a bandlimited function in k-space. We denote by \mathcal{A} the shift invariant (SI) subspace of bandlimited functions in k-space, $f \in \mathcal{A}$, spanned by

$$\mathbf{a}_n(k) = \text{sinc}((k - \Delta n)/\Delta), \quad (1)$$

with spacing Δ in the k-space corresponding to $\text{FOV} \triangleq 1/\Delta$ in the image space and $n \in \mathbb{Z}$. For computational purposes we use a finite subspace, $n = 1, \dots, N$, which approximates the space of bandlimited functions.

We seek an efficient solution to the reconstruction problem: Given \mathbf{b} , a set of nonuniformly spaced samples of an unknown $f \in \mathcal{A}$, $\{f(\kappa_m)\}, m = 1, \dots, M$, find a good approximation $\hat{f}(k_n)$ on a given set of uniformly spaced sampling points $\{k_n\}, n = 1, \dots, N$, from which we can subsequently reconstruct the image $F(x)$ by using the efficient IFFT.

In the next sections concepts from the function-space approach to sampling theory are presented, followed by their application to MRI imaging as manifested by the new GSURS algorithm.

III. GENERALIZED-SAMPLING APPROACH CONCEPTS

In the classic approach to signal sampling the signal f is represented by measurements which are its values at given sampling points. In recent years [8]–[10] this idea was expanded and generalized within a function-space framework. The processes of sampling and reconstruction can be viewed as an expansion of a signal onto a set of vectors that span a signal space. Suppose that a signal f lies in an arbitrary subspace \mathcal{A} of a Hilbert space \mathcal{H} . It can be represented by

$$f = \sum_{n=1}^N d[n] \mathbf{a}_n = A\mathbf{d},$$

where $\mathbf{d} \in \mathbb{C}^N$, and $A : \mathbb{C}^N \rightarrow \mathcal{H}$ is a set transform corresponding to vectors $\{\mathbf{a}_n\}, n = 1, \dots, N$ which span the subspace \mathcal{A} and constitute a Riesz basis or a frame [11]. Thus, applying A is equivalent to taking linear combinations of the set of vectors $\{\mathbf{a}_n\}$.

Measurements are expressed as inner products of the function to be sampled f with a set of vectors $\{\mathbf{s}_m\}, m = 1, \dots, M$ that span the sampling subspace $\mathcal{S}_N \subseteq \mathcal{H}$. Using this notation, the vector of samples \mathbf{b} is given by $\mathbf{b} = S_N^* f$ where $b[m] = \langle \mathbf{s}_m, f \rangle$ and S_N^* is the adjoint of S_N .

As shown in [12], a consistent approximation of f can be recovered in \mathcal{A} from its samples using an oblique projection:

$$\hat{f} = E_{AS_N^\dagger} f = A(S_N^* A)^\dagger S_N^* f, \quad (2)$$

where \dagger denotes the pseudoinverse. The geometrical interpretation of this reconstruction scheme is illustrated in Fig. 1(a). When certain conditions are fulfilled, $S_N^* A$ is invertible and perfect reconstruction is attained, $\hat{f} = f$.

IV. GENERALIZED SPARSE UNIFORM RESAMPLING ALGORITHM

In MRI we are given a set of M nonuniformly spaced samples in 2D or 3D k-space of a signal $f \in \mathcal{A}$, where \mathcal{A} is a subspace of bandlimited functions spanned by a_n defined in (1). The samples are given by $b[m] = \langle \mathbf{s}_m, f \rangle$, where $\mathbf{s}_m(k) = \delta(k - \kappa_m)$ spans the sampling subspace \mathcal{S}_N . The solution given in (2) can be shown to be equivalent to the URS scheme [3], where the pseudoinverse of the full matrix

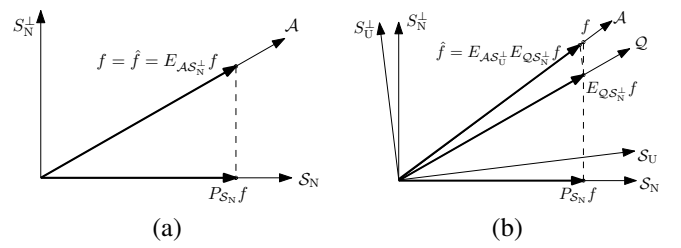


Fig. 1. Geometrical interpretation of: (a) An oblique projection in a perfect reconstruction scenario; (b) The GSURS scheme.

$S_N^* A$ is calculated and used to recover the values of $f(k)$ on the uniform grid. For a 2D or 3D MRI image, storing $S_N^* A$ on the computer, not to mention calculating $(S_N^* A)^\dagger$, is intractable due to the sheer size the matrices involved. Even if we were given $(S_N^* A)^\dagger$ and were able to store it, calculating $\mathbf{d} = (S_N^* A)^\dagger \mathbf{b}$ requires $O(N \times M)$ complex operations, which is by and large computationally prohibitive.

The method described herein for reconstruction from nonuniformly spaced samples employs a generalized sampling scheme. By cleverly selecting an intermediate reconstruction subspace \mathcal{Q} , we show that a sparse system of equations is produced that can be solved efficiently using solvers for sparse linear equations. The resulting reconstruction process is performed with only a minor increase in the approximation error.

We begin by introducing an intermediate subspace $\mathcal{Q} \in \mathcal{H}$ which is spanned by a set of vectors $\{q_n\}$, which are integer translations of a compactly supported function $q(k)$, i.e., $q_n(k) = q((k - \Delta n)/\Delta)$ where $n = 1, \dots, N$. It is straightforward to extend this 1D notation into higher dimension using separable functions. We define a resampling subspace \mathcal{S}_U spanned by $u_n(k) = \delta(k - k_n)$, where $\{k_n\}, n = 1, \dots, N$ are the uniformly spaced sampling points. Our reconstruction process comprises a sequence of two oblique projections, as described by the following equation:

$$\hat{f} = \underbrace{A(S_U^* A)^\dagger}_{E_{AS_U^\dagger}} \underbrace{S_U^* Q(S_N^* Q)^\dagger}_{E_{QS_N^\dagger}} S_N^* f. \quad (3)$$

The geometrical interpretation of (3) is depicted in Fig. 1(b). We name the resulting reconstruction process the Generalized Sparse Uniform ReSampling (GSURS) algorithm.

Let us split the sequence of operators in (3) into two parts. Define

$$\mathbf{c} = (S_N^* Q)^\dagger \mathbf{b}, \quad (4)$$

where \mathbf{c} , is a vector of N generalized samples of f on a uniformly spaced grid, and

$$\mathbf{d} = (S_U^* A)^\dagger (S_U^* Q) \mathbf{c}. \quad (5)$$

In order to calculate \mathbf{c} let us first reformulate relation (4) as $\mathbf{b} = S_N^* Q \mathbf{c}$, which for $\mathbf{s}_m(k) = \delta(k - \kappa_m)$ can be described by the following set of equations:

$$b[m] = \sum_{n=1}^N c[n] q(\kappa_m - k_n). \quad (6)$$

Due to the compact support of q , only a small number of coefficients $c[n]$ in (6) contribute to the calculation of each value $b[n]$. Therefore, (6) represents a sparse relation between the coefficient vectors \mathbf{b} and \mathbf{c} , which can be expressed by a $M \times N$ sparse matrix Φ , with elements:

$$\{\Phi\}_{m,n} = \{S_N^* Q\}_{m,n} = q(\kappa_m - k_n).$$

This equation, $\mathbf{b} = \Phi \mathbf{c}$, is solved using the weighted regularized least squares:

$$\mathbf{c} = \arg \min_{\mathbf{c}'} \|\bar{\Gamma} (\Phi \mathbf{c}' - \mathbf{b})\|^2 + \rho \|\mathbf{c}'\|^2. \quad (7)$$

A useful sparsity conserving formulation for the normal equation which solves (7) employs the ‘‘sparse tableau’’ approach [13]:

$$\begin{pmatrix} \bar{\Gamma} \mathbf{b} \\ \mathbf{0} \end{pmatrix} = \begin{pmatrix} \mathbf{I} & \bar{\Gamma} \Phi \\ \Phi^T \bar{\Gamma}^T & -\rho^2 \mathbf{I} \end{pmatrix} \begin{pmatrix} \mathbf{r} \\ \mathbf{c} \end{pmatrix}, \quad (8)$$

where ρ is a regularization scalar, \mathbf{r} is the residual from (7) which is minimized, and $\bar{\Gamma} = \Gamma^{\frac{1}{2}}$, where Γ is a diagonal weighting matrix with weights $\gamma_i > 0$. The sparse system matrix in (8) is denoted Ψ .

This system of equations is solved using a sparse direct solver which calculates the LU decomposition of Ψ . In particular, the matrix Ψ is factored as: $\mathbf{P} (\mathbf{R}^{-1} \Psi) \mathbf{Q} = \mathbf{L} \mathbf{U}$, where \mathbf{P} and \mathbf{Q} are permutation matrices, \mathbf{R} is a diagonal weighting matrix, and \mathbf{L} and \mathbf{U} are lower and upper triangular matrices respectively. For further details refer to [14]. We emphasize that the factorization process is performed offline only once for a given sampling trajectory and does not need to be repeated for each new sampling data set. Given samples \mathbf{b} , the solution of the sparse system of equations is performed online by forward substitution and backward elimination. This operation typically achieves linear memory usage and computational complexity of $O(N_{\text{NZ}})$, where N_{NZ} is the number of non-zero elements in the matrix Ψ .

Once the vector of uniformly spaced generalized samples \mathbf{c} is calculated according to (4), we proceed to calculate the uniformly spaced k-space samples \mathbf{d} from (5). Since both \mathbf{c} and \mathbf{d} are located on a uniformly spaced grid and in addition, \mathcal{Q} and \mathcal{A} are SI subspaces, (5) can be performed efficiently using a linear shift-invariant (LSI) filter. As shown in [8], the filter is described by:

$$H_{\text{COR}}(e^{j\omega}) = \begin{cases} \frac{R_{S_U \mathcal{Q}}(e^{j\omega})}{R_{S_U \mathcal{A}}(e^{j\omega})}, & R_{S_U \mathcal{A}}(e^{j\omega}) \neq 0 \\ 0, & R_{S_U \mathcal{A}}(e^{j\omega}) = 0 \end{cases}. \quad (9)$$

Given the reconstructed uniformly spaced k-space samples $\mathbf{d} = \hat{f}(k_n)$, the reconstruction process is completed by transforming back into the image domain $\mathbf{e} = \text{IFFT}\{\mathbf{d}\}$. The estimate of the uniformly sampled image is then given by $\hat{F}(x_n) = |e[n]|$. The entire reconstruction process, including the series of projections followed by the IFFT, can be implemented by the system depicted in Fig. 2.

We note that rather than performing the filtering operation (9) in k-space, it can be implemented efficiently as an element-wise product in the image domain – following the IFFT.

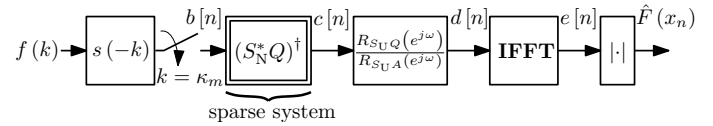


Fig. 2. GSURS system block diagram.

The approximation error in the reconstruction process can be reduced by resampling onto a denser uniform grid in k-space. This is done by scaling Δ in Eq. (1) by a factor $I > 1$, i.e., $\tilde{\Delta} = \Delta/I$, thereby increasing N by a factor of I^{dim} , where dim is the dimension of our problem. Increasing I reduces the approximation error with a penalty of increasing the computational load. The selection of $q(k)$, both the function itself and its support, affects the quality of the reconstructed image. For example, when using a B-spline kernel, increasing the degree of the spline improves the image quality at the expense of increased computational burden.

When implementing the algorithm, the process is divided into two phases. The first phase is performed offline only once for a given sampling trajectory, while the second is an online phase which is repeated for each new set of samples. In the offline phase, all the data structures are prepared and the ‘‘sparse tableau’’ system matrix Ψ is factorized. In the online phase the sparse system is solved using forward substitution and backward elimination for a given set of samples \mathbf{b} . The result is filtered using H_{COR} , and IFFT followed by an absolute value is performed to obtain the final image.

It can be shown that the online computational load is similar to that of CG and of a single iteration of the NUFFT.

V. GSURS ALGORITHM SUMMARY

In this section we summarize the GSURS algorithm. The algorithm is divided into two stages. The first is the offline stage which is performed only once for a given sampling trajectory, and the second is an online stage which is repeated for each new set of samples.

Algorithm inputs: Sampled values \mathbf{b} and corresponding nonuniform k-space locations $\{\kappa_j\}$, and k-space uniform locations $\{k_i\}$.

Phase 1 - Offline preparation and factorization: all

the data structures are prepared according to given nonuniform sampling and uniform reconstruction grids and a given compactly supported kernel $q(\cdot)$. Given a chosen regularization scalar ρ and a diagonal weighting matrix Γ , the ‘‘sparse tableau’’ system matrix Ψ is prepared and factorized. See Algorithm 1.

Phase 2 - Online solution: using the outputs of the previous phase, the sparse system of equations is solved for a given set of k-space samples \mathbf{b} . The result is subsequently filtered using the precomputed digital correction filter $H_{\text{COR}}(e^{j\omega})$ producing the uniformly spaced samples \mathbf{d} . These, in turn, are transformed into image space using the IFFT. See Algorithm 2.

Algorithm outputs: Uniformly spaced k-space samples \mathbf{d} and reconstructed image $\hat{F}(x_n) = |e[n]|$.

Input:

- $\{\kappa_j, j = 1, \dots, M\}$: nonuniform sampling grid in k-space.
- $\{k_i, i = 1, \dots, N\}$: uniform reconstruction grid in k-space.
- $q(\cdot)$: a compactly supported kernel (e.g. β -spline).
- $\mathbf{\Gamma}$: a $N \times N$ diagonal weighting matrix, $\bar{\mathbf{\Gamma}} = \mathbf{\Gamma}^{\frac{1}{2}}$.
- ρ : a regularization scalar.

Algorithm:

1: Construct the sparse system matrix Φ , where $\{\Phi\}_{m,n} = q(\kappa_m - k_n)$.

2: Calculate the LSI filter to be used for correction:

$$H_{COR}(e^{j\omega}) = \frac{R_{SQ}(e^{j\omega})}{R_{SA}(e^{j\omega})}$$

3: Construct the “sparse tableau” system matrix:

$$\Psi = \begin{pmatrix} \mathbf{I} & \bar{\mathbf{\Gamma}}\Phi \\ \Phi^T \bar{\mathbf{\Gamma}}^T & -\rho^2 \mathbf{I} \end{pmatrix}$$

4: Factorize Ψ so that $\mathbf{P}(\mathbf{R}^{-1}\Psi)\mathbf{Q} = \mathbf{L}\mathbf{U}$.

Output: $H_{COR}(e^{j\omega})$ and $\mathbf{L}, \mathbf{U}, \mathbf{P}, \mathbf{Q}, \mathbf{R}$.

Algorithm 1: GSURS - “Offline preparation and factorization”

Input:

- $\mathbf{L}, \mathbf{U}, \mathbf{P}, \mathbf{Q}, \mathbf{R}$.
- \mathbf{b} : a $M \times 1$ vector of nonuniformly spaced “raw data” k-space sample values of f , where $b_j = f(\kappa_j)$.
- $\mathbf{H}_{COR}(e^{j\omega})$

Algorithm:

1: Scale \mathbf{b} by \mathbf{R} and permute the result using \mathbf{P} . Store it in the full length vector $\mathbf{y} = \mathbf{P}(\mathbf{R}^{-1}\mathbf{b})$.

2: Solve $\mathbf{Lz} = \mathbf{y}$ and $\mathbf{Uw} = \mathbf{z}$ by forward and backward substitutions.

3: Permute \mathbf{w} by \mathbf{Q} and store the results in \mathbf{c} ($\mathbf{c} = \mathbf{Q}\mathbf{w}$).

4: Filter \mathbf{c} using $H_{COR}(e^{j\omega})$ and store the results in \mathbf{d} .

5: Compute $\mathbf{e} = \text{IFFT}\{\mathbf{d}\}$.

Output: \mathbf{d} and the image $\hat{F}(x_n) = |e[n]|$.

Algorithm 2: GSURS - “Online solution”

The computational complexity of the “Online solution” phase of the algorithm, the phase performed for each new acquired set of samples, can be shown to be:

$$O\left(M(q_{\text{sup}}I)^2 + N^2(1 + I^2 \log(NI))\right),$$

where M and N are the number of nonuniform and uniform grid points, respectively, I is the over sampling factor and q_{sup} is the support of the compactly supported kernel $q(\cdot)$. It can be shown that this computational load is similar to that of CG and of a single iteration of the NUFFT.

VI. NUMERICAL SIMULATION

Computer simulations are used to compare the performance of the GSURS algorithm with that of CG [2] and the NUFFT

algorithm [5] employing the “NFFT” package [15]. A standard numerical Shepp-Logan Phantom [16] of dimensions 256×256 is used. This phantom has been used extensively for numerical simulations both in CT and in MRI [17]. The phantom is sampled using a radial trajectory [18] with $N_{\text{spokes}} = 60$, where N_{spokes} is the number of spokes and $N_{\text{points}} = 512$, where N_{points} is the number of sample points along each spoke so that $M = N_{\text{spokes}} \cdot N_{\text{points}}$. White Gaussian noise (WGN) is added to the samples.

CG reconstruction is performed using a Kaiser-Bessel window with β chosen according to [2]. The NUFFT uses a Kaiser-Bessel window with $m = 6$, corresponding to a window width of 13 samples. The NUFFT and CG methods use density compensation weights. GSURS uses a B-spline of degree $p = 3$ which corresponds to a support of 4 samples. All the reconstruction methods use an over-sampling factor of $I = 2$.

For each experiment the root-mean-square error (RMSE) of the reconstructed image is calculated with respect to the original phantom. The RMSE between a vector \mathbf{y} and its estimate $\hat{\mathbf{y}}$ is defined by:

$$\text{RMSE}(y, \hat{y}) \triangleq \frac{\|y - \hat{y}\|_2}{\|y\|_2}.$$

In the first experiment various levels of complex WGN are added to the samples, and the RMS error is calculated for each reconstruction. The results are depicted in Fig. 3.

It can be seen that GSURS exhibits the best performance, with CG showing the poorest performance. A single iteration of NUFFT yields similar results to CG; increasing the number of iterations improves the results. In our experiments we observed that when using a large number of iterations (> 10), NUFFT showed similar performance to GSURS.

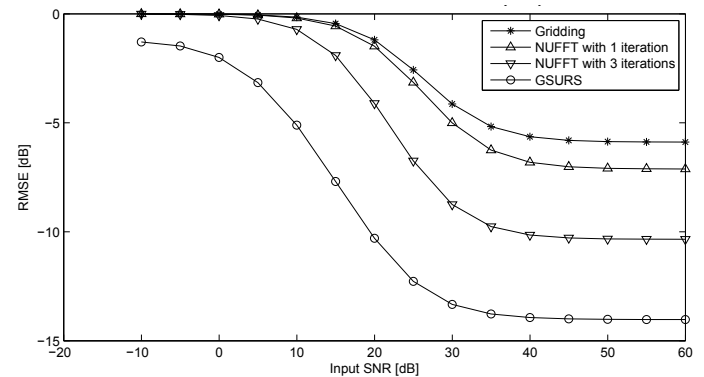


Fig. 3. Reconstruction RMSE as a function of input SNR. Shepp-Logan phantom using a radial trajectory, $M=30720$, $N=65536$

Fig. 4 compares the reconstruction methods for input SNR of 60dB (corresponding to the rightmost points in Fig. 3). The resulting image is depicted alongside two profiles within the image: a horizontal profile along row 128 and a vertical profile along column 160. The quality of reconstruction of the different methods is clearly exhibited in the profile plots.

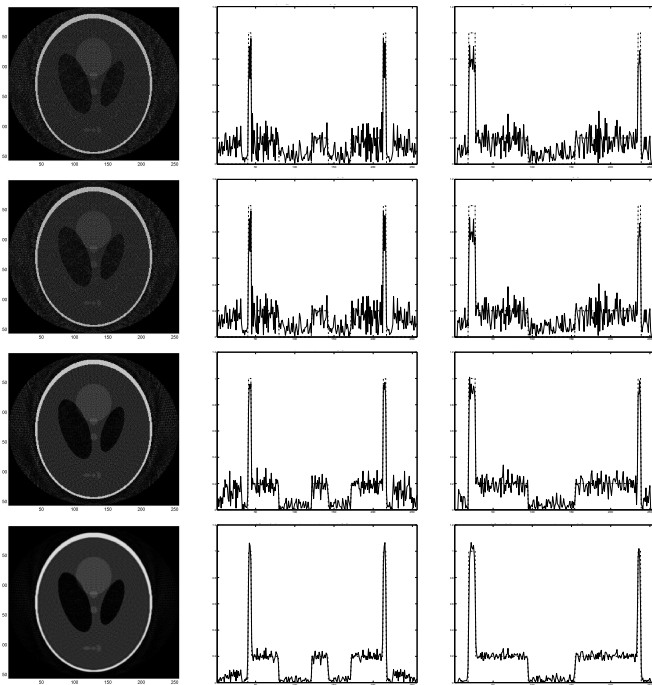


Fig. 4. Reconstructed images and profiles for $i\text{SNR} = 60$ dB and $M=30720$. First row - CG. Second row - NUFFT 1 iteration. Third row - NUFFT 3 iterations. Forth row - GSURS.

In the final experiment the performance of the reconstruction process is tested while decreasing the total number of samples (M). It is expected that the quality of reconstruction will deteriorate as M is reduced. As expected, Fig. 5 shows this decline in performance, however GSURS maintains its performance advantage over the entire range and exhibits a slower rate of performance degradation.

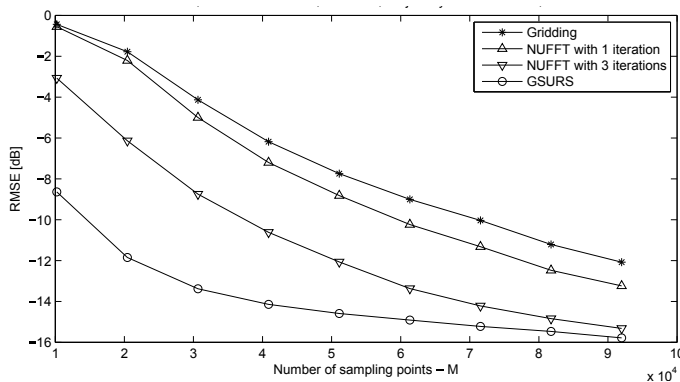


Fig. 5. Shepp-Logan phantom with radial trajectory, input SNR = 30dB, $N=65536$; RMS error as a function of M .

VII. CONCLUSION

A new method for reconstruction of images from nonuniformly spaced k -space samples is presented which derives from modern sampling theory. A sequence of projections is performed, with the introduction of an interim subspace comprising of integer shifts of a compactly supported kernel.

This allows us to construct a sparse set of linear equations, enabling us to exploit efficient sparse equation solvers resulting in a considerable reduction in the computational cost. After performing the offline data preparation step, the computational burden of the online stage is comparable with that of CG or of a single iteration of NUFFT.

In terms of the quality of the reconstructed images, it is demonstrated that the performance of the new algorithm exceeds that of both CG and NUFFT with 1-3 iterations. In our experiments we observed that multiple iterations of NUFFT gradually converge to similar results, however, with the penalty of an increased computational load.

REFERENCES

- [1] H. Schomberg and J. Timmer, "The gridding method for image reconstruction by Fourier transformation," *IEEE Transactions on Medical Imaging*, vol. 14, no. 3, pp. 596–607, 1995.
- [2] J. I. Jackson, C. H. Meyer, D. G. Nishimura, and A. Macovski, "Selection of a convolution function for Fourier inversion using gridding [computerized tomography application]," *IEEE Transactions on Medical Imaging*, vol. 10, no. 3, pp. 473–478, 1991.
- [3] D. Rosenfeld, "An optimal and efficient new gridding algorithm using singular value decomposition," *Magnetic Resonance in Medicine*, vol. 40, no. 1, pp. 14–23, 1998.
- [4] —, "New approach to gridding using regularization and estimation theory," *Magnetic resonance in medicine*, vol. 48, no. 1, pp. 193–202, 2002.
- [5] A. Dutt and V. Rokhlin, "Fast Fourier transforms for nonequispaced data," *SIAM Journal on Scientific computing*, vol. 14, no. 6, pp. 1368–1393, 1993.
- [6] J. Song, Q. H. Liu, S. L. Gewalt, G. Cofer, and G. A. Johnson, "Least-square nufft methods applied to 2-d and 3-d radially encoded mr image reconstruction," *Biomedical Engineering, IEEE Transactions on*, vol. 56, no. 4, pp. 1134–1142, 2009.
- [7] N. Nguyen and Q. H. Liu, "The regular Fourier matrices and nonuniform fast Fourier transforms," *SIAM Journal on Scientific Computing*, vol. 21, no. 1, pp. 283–293, 1999.
- [8] Y. C. Eldar, *Sampling Theory: Beyond Bandlimited Systems*. Cambridge University Press, 2015.
- [9] M. Unser and A. Aldroubi, "A general sampling theory for nonideal acquisition devices," *IEEE Transactions on Signal Processing*, vol. 42, no. 11, pp. 2915–2925, 1994.
- [10] M. Unser, "Sampling—50 years after Shannon," *Proceedings of the IEEE*, vol. 88, no. 4, pp. 569–587, 2000.
- [11] I. Daubechies, "The wavelet transform, time-frequency localization and signal analysis," *IEEE Transactions on Information Theory*, vol. 36, no. 5, pp. 961–1005, 1990.
- [12] Y. C. Eldar, "Sampling with arbitrary sampling and reconstruction spaces and oblique dual frame vectors," *Journal of Fourier Analysis and Applications*, vol. 9, no. 1, pp. 77–96, 2003.
- [13] M. T. Heath, "Numerical methods for large sparse linear least squares problems," *SIAM Journal on Scientific and Statistical Computing*, vol. 5, no. 3, pp. 497–513, 1984.
- [14] T. A. Davis, "Algorithm 832: Umfpack v4. 3—an asymmetric-pattern multifrontal method," *ACM Transactions on Mathematical Software (TOMS)*, vol. 30, no. 2, pp. 196–199, 2004.
- [15] J. Keiner, S. Kunis, and D. Potts, "Using NFFT 3—a software library for various nonequispaced fast Fourier transforms," *ACM Transactions on Mathematical Software (TOMS)*, vol. 36, no. 4, p. 19, 2009.
- [16] L. A. Shepp and B. F. Logan, "The Fourier reconstruction of a head section," *IEEE Transactions on Nuclear Science*, vol. 21, no. 3, pp. 21–43, 1974.
- [17] M. Guerquin-Kern, F. I. Karahanoglu, D. Van De Ville, K. P. Pruessmann, and M. Unser, "Analytical form of shepp-logan phantom for parallel mri," in *Biomedical Imaging: From Nano to Macro, 2010 IEEE International Symposium on*. IEEE, 2010, pp. 261–264.
- [18] V. Rasche, R. W. D. Boer, D. Holz, and R. Proksa, "Continuous radial data acquisition for dynamic MRI," *Magnetic resonance in medicine*, vol. 34, no. 5, pp. 754–761, 1995.